Appl Microbiol Biotechnol
DOI 10.1007/s00253-015-6541-1

Concatemerization increases the inhibitory activity of short, cell-penetrating, cationic and tryptophan-rich antifungal peptides

Belén López-García[1] · Eleonora Harries[2] · Lourdes Carmona[2] · Lidia Campos-Soriano[1] · José Javier López[3] · Paloma Manzanares[3] · Mónica Gandía[2] · María Coca[1] · Jose F. Marcos[2]

Received: 12 January 2015 / Revised: 5 March 2015 / Accepted: 9 March 2015

Abstract There are short cationic and tryptophan-rich antifungal peptides such as the hexapeptide PAF26 (RKKWFW) that have selective toxicity and cell penetration properties against fungal cells. This study demonstrates that concatemeric peptides with tandem repeats of the heptapeptide PAF54 (which is an elongated PAF26 sequence) show increased fungistatic and bacteriostatic activities while maintaining the absence of hemolytic activity of the monomer. The increase in antimicrobial activity of the double-repeated PAF sequences (diPAFs), compared to the nonrepeated PAF, was higher (4–8-fold) than that seen for the triple-repeated sequences (triPAFs) versus the diPAFs (2-fold). However, concatemerization diminished the fungicidal activity against quiescent spores of the filamentous fungus *Penicillium digitatum*. Peptide solubility and sensitivity to proteolytic degradation were affected by the design of the concatemers: incorporation of the AGPA sequence hinge to separate PAF54 repeats increased solubility while the C-terminal addition of the KDEL sequence decreased in vitro stability. These results led to the design of the triPAF sequence PAF102 of 30 amino acid residues, with increased antimicrobial activity and minimal inhibitory concentration (MIC) value of 1–5 μM depending on the fungus. Further characterization of the mode-of-action of PAF102 demonstrated that it colocalizes first with the fungal cell wall, it is thereafter internalized in an energy dependent manner into hyphal cells of the filamentous fungus *Fusarium proliferatum*, and finally kills hyphal cells intracellularly. Therefore, PAF102 showed mechanistic properties against fungi similar to the parental PAF26. These observations are of high interest in the future development of PAF-based antimicrobial molecules optimized for their production in biofactories.

Keywords Antimicrobial · Antifungal peptide · Cell-penetrating peptide · Phytopathogen · Fungal cell wall

Belén López-García and Eleonora Harries contributed equally to this work.

Electronic supplementary material The online version of this article (doi:10.1007/s00253-015-6541-1) contains supplementary material, which is available to authorized users.

✉ María Coca
maria.coca@cragenomica.es

✉ Jose F. Marcos
jmarcos@iata.csic.es

[1] Centre for Research in Agricultural Genomics (CRAG), CSIC-IRTA-UAB-UB. Edifici CRAG, Campus UAB, 08193 Bellaterra, Barcelona, Spain

[2] Food Science Department, Instituto de Agroquímica y Tecnología de Alimentos (IATA) - CSIC, Avda. Agustín Escardino 7, Paterna 46980, Valencia, Spain

[3] Biotechnology Department, Instituto de Agroquímica y Tecnología de Alimentos (IATA) - CSIC, Avda. Agustín Escardino 7, Paterna 46980, Valencia, Spain

Introduction

Antimicrobial peptides (AMPs) and proteins are widespread in nature in organisms from microbes to animals (Jenssen et al. 2006; Zasloff 2002). In higher organisms, AMPs are part of ancient defense mechanisms against pathogenic microbes while in microbes act in the competition for nutrient resources. AMPs differ in length (less than 100 residues), sequence, and structure, but most are cationic and amphipathic. The fast and efficient action of AMPs against microbes and the low toxicity to mammalian and plant cells have attracted attention to AMPs as a novel class of antibiotics, with potential

application in medicine, crop protection, and food preservation (Cotter et al. 2005; De Lucca and Walsh 1999; De Souza Cândido et al. 2014; Hancock and Sahl 2006; López-García et al. 2012; Marcos et al. 2008; Montesinos and Bardaji 2008). The short length of AMPs enables the rational design of sequence modifications that modulate and improve their antimicrobial and therapeutic properties, such as potency, specificity, bioavailability, or stability.

PAF26 (amino acid sequence RKKWFW) is a synthetic de novo-designed hexapeptide that was identified in a combinatorial screen against the phytopathogen *Penicillium digitatum* and shares sequence similarity with other AMP from natural or synthetic origin (reviewed in Muñoz et al. 2013a). Additional examples of fungi that have been demonstrated to be sensitive to PAF26 and PAF26 derivatives include the phytopathogens *Penicillium italicum*, *Penicillium expansum*, *Botrytis cinerea*, and *Fusarium oxysporum* (López-García et al. 2002, 2003); the human pathogens *Candida albicans*, *Aspergillus fumigatus*, and several dermatophytes (López-García et al. 2007; Muñoz et al. 2013b); and the model fungus *Neurospora crassa* (Muñoz et al. 2012). PAF26 is a cationic tryptophan-rich peptide that belongs to the cell-penetrating class of AMPs (CP-AMPs). Penetration into fungal cells has been analyzed in detail using live-cell imaging techniques in the model filamentous fungus *N. crassa* (Muñoz et al. 2012). The study demonstrated energy-dependent endocytic internalization of PAF26 prior to killing fungal cells. Therefore, PAF26 possesses the determinants for both antifungal and cell-penetrating activities in just six amino acid residues, and we have proposed it as a useful model to analyze these two activities as well as the relationships between them.

A crucial question for the exploitation of short AMP is their cost-effective production (Duncan and O'Neil 2013). Synthetic procedures are viable for the high added value of medical usage. Other applications might require the use of biotechnological approaches and heterologous expression of synthetic genes in bacteria, fungal, or plant biofactories (Ingham and Moore 2007; Parachin et al. 2012). Specific challenges for the biotechnological production of short AMPs in cell factories are their small length, susceptibility to degradation, and potential toxicity to the producer host. Fusion to other protein motifs has been used to stabilize AMP in the producer host (Company et al. 2014; Viana et al. 2013; Wang et al. 2014) or to target AMP to cell compartments such as the endoplasmic reticulum (ER) or protein bodies (Bundó et al. 2014; Coca et al. 2006; Company et al. 2014) where they can accumulate in high amounts.

Size increase of AMP is an attractive approach to improve peptide production in biofactories for several reasons. Increased size is expected to enhance stability of very short peptides. Fusions of different AMP sequences into single peptides have been shown to result in new AMPs with enhanced properties (Ferre et al. 2006; López-García et al. 2007; Piers et al. 1994). Additionally, size increase could produce more active molecules on a molar basis, as demonstrated in the case of concatemer elongation of the antibacterial peptide BP100 (Badosa et al. 2013) or the antifungal series of (RW)n or (KW)n repeats with increasing "n" number (Gopal et al. 2012).

In the first part of this study, the properties of series of peptides that are tandem repeats of different size and design derived from the PAF26 sequence have been characterized, in terms of antimicrobial activity, nonspecific lytic toxicity, and stability to protease degradation. In a second part, a triple-repeated sequence that shows improved antimicrobial activity over PAF26 was designed and demonstrated to act by cell penetration into fungal cells in an energy-dependent and non-disruptive way.

Materials and methods

Microorganisms and media

The microorganisms used in this study were reference strains from diverse fungi of agricultural relevance: *P. digitatum* CECT20796, *F. oxysporum* 4287 (Di Pietro and Roncero 1996) (provided by Dr. M. I. G. Roncero, Universidad de Córdoba, Córdoba, Spain), *B. cinerea* CECT2100, and *Magnaporthe oryzae* PR-9 (Coca et al. 2004) (CIRAD collection, Montpellier, France). Additionally, a *Fusarium proliferatum* local isolate collected from rice plants (provided by the Plant Protection Facilities of the Generalitat de Catalunya, Barcelona, Spain) and a transformant derived from it that constitutively accumulates the green fluorescent protein (GFP-Fp) were used. GFP-Fp was obtained by *Agrobacterium tumefaciens*-mediated transformation as described (Campos-Soriano and San Segundo 2009). The plasmid used for transformation contains the *eGFP* gene under the control of the glyceraldehyde-3-phosphate dehydrogenase promoter from *Agaricus bisporus* and the CaMV 35S terminator (Chen et al. 2000). Fungi were cultured on potato dextrose agar (PDA) (Difco-BD Diagnostics, Sparks, MD, USA) plates at 24 °C with the exception of *M. oryzae*, which was maintained on rice flour medium. Conidia (mitotic asexual spores) were collected and adjusted to the appropriate concentration. The Gram-negative bacterium *Escherichia coli* DH5α (Invitrogen, Eugene; OR, USA) was also used and grown in Luria-Bertani (LB) medium at 37 ° C.

Synthetic peptides

All the peptides used were synthetic and purchased from GenScript (Piscataway, NJ, USA) at ≥95 % purity. The sequences of the PAF peptides used are listed in Table 1. Peptide PAF102 was also synthesized labeled by covalent modification of the N-terminus with tetramethyl-rhodamine (TMR-P102). Additional synthetic peptides used as controls in the hemolytic assays were as follows: the natural cytolytic peptide melittin (GIGAVLKVLTTGLPALISWIKRKRQQ) from honeybee venom (Dempsey 1990), the rationally designed heptapeptide 77-3 (FRLKFHF) (Gonzalez et al. 2002), and the active fragment P113 (AKRHHGYKRKFH) from human histatin 5, a natural cell-penetrating antifungal peptide isolated from human saliva (Jang et al. 2008). Stock solutions of peptides were prepared at 1-5 mM in 10 mM 3-(N-morpholino)-propanesulfonic acid (MOPS) (Sigma-Aldrich, St. Louis, MO, USA), pH 7 buffer and stored at −20 °C. Peptide concentrations were determined spectrophotometrically (López-García et al. 2002).

Antimicrobial activity assays

Growth inhibition assays were carried out in 96-well microtiter plates essentially as described (López-García et al. 2002) with minor modifications. A volume of 90 μL of fungal conidia (or bacterial cells) in appropriate growth media, 1/20 diluted potato dextrose broth (PDB) (Difco-BD Diagnostics) for fungi or 1/10 diluted LB for bacteria, was mixed in each plate well with 10 μL of 10× concentrated peptide solution from serial 2-fold dilutions. All samples were prepared in triplicate. Plates were statically incubated for 48 h at the temperature optimal for each fungus or bacteria. Growth was measured every 2 h at OD_{600} using a Multiskan Spectrum plate spectrophotometer (Thermo Electron Corporation, Vantaa, Finland). Dose-response curves were generated from measurements after 48 h. Experiments summarized in Table 1 were conducted two to four times for each peptide/microorganism combination. The minimal inhibitory concentration (MIC) is the peptide concentration that completely inhibited growth in all the experiments carried out.

A solubility index (SI, Table 1) as indicator of solubility of peptides under the antimicrobial testing conditions was recorded by the appearance of turbidity (i.e., OD_{600}, optical density at 600 nm above the background value of 0.05) of LB solutions (in the absence of bacteria) containing peptides at 16 μM (SI score 3), 32 μM (score 2), or 64 μM (score 1) (see Table 1).

Fungicidal activity was assessed by incubating nongerminated conidia of *P. digitatum* with peptides at either 16 or 64 μM in water for 16 h and then plating dilutions to determine conidia viability as described (Muñoz et al. 2007a).

Hemolytic assays

The hemolytic activity of the peptides was determined on human red blood cells essentially as described (Muñoz et al. 2006). No hemolysis and 100 % hemolysis were determined in controls with PBS and 0.1 % Triton X-100, respectively. The hemolytic activity of each peptide was calculated as the percentage of total hemoglobin released (detected as absorbance at 415 nm) compared with that released by incubation with 0.1 % Triton X-100.

Proteolytic digestion assays

Peptides (5 μM) dissolved in 10 mM MOPS pH 7 were digested with 5 μg/mL of recombinant proteinase K (approximately 2.0 U/mg) (Roche, Mannheim, Germany) at 30 °C. Aliquots were withdrawn from the reaction mixtures at 0, 15, 30, 60, and 120 min and immediately heated at 80 °C for 10 min in a water bath to inactivate the enzyme. Each sample was stored at −20 °C until further analysis by reversed-phase high-performance liquid chromatography (RP-HPLC). Digestions were performed in duplicate, and the experiment was repeated twice.

Analysis of digests by RP-HPLC was performed using a Waters system (Waters Corporation, Milford, MA, USA) equipped with a 1525 Binary HPLC pump, a 2996 Photodiode Array Detector and a 717 plus Autosampler. A Symmetry C18 column (4.6×150 mm, 5 μm, Waters) kept at 40 °C was operated at a flow rate of 1 mL/min. Peptides were eluted with a linear gradient of solvent B (acetonitrile with 0.1 % TFA) in solvent A (water with 0.1 % TFA) from 0 to 40 % in 20 min and detected at 214 nm.

Fluorescence microscopy

GFP-Fp (10^6 spores/mL) was germinated in 1/10 diluted PDB for 4–5 h at 28 °C. Then, aliquots of 8 μL were mixed with 2 μL of 25 μM TMR-PAF102. For some experiments, germinated fungus was stained with the chitin-binding dye calcofluor white (CFW) (Fluka, Buchs, Switzerland) at a final concentration of 50 μg/mL before peptide treatment. To determine if peptide internalization is energy-dependent, germinated fungus was pretreated with 3 mM sodium azide (NaN_3) (Fluka) for 15 min.

Confocal laser scanning microscopy was performed using an Olympus FV1000 microscope (Tokyo, Japan). TMR-PAF102 was excited at 559 nm, and the emission window was set at 575–675 nm. GFP was excited with an argon ion laser emitting at 488 nm and fluorescence detected at 500–545 nm. CFW was excited at 405 nm and fluorescence detected at 410–450 nm. Simultaneous bright-field images were captured with a transmitted light detector.

Table 1 Amino acid sequences, properties, and growth inhibitory activity of peptides used in this study

Peptide	Sequence[a]	#AA	MW[b]	Charge[c]	pI[b]	GRAVY[b]	*Pdig*[d]	*Mory*[d]	*Foxy*[d]	*Bcin*[d]	*Ecol*[e]	SI[f]
PAF54	HRKKWFW	7	1087.3	+3.1	11.2	−2.07	16	>32	32	16	32	
PAF55	HRKKWFWKDEL	11	1572.8	+2.1	9.7	−1.96	32			32	128	
PAF56	GHRKKWFW	8	1144.3	+3.1	11.2	−1.86	16			32		
PAF57	SHRKKWFW	8	1174.2	+3.1	11.2	−1.91	16			16		
PAF58	GHRKKWFWKDEL	12	1629.8	+2.1	9.7	−1.83	32		>32		>128	
PAF59	SHRKKWFWKDEL	12	1659.9	+2.1	9.7	−1.87	32		>32		>128	
PAF60	HRKKWFWAGPAHRKKWFW	18	2452.9	+6.2	12.8	−1.52	2	16		2	8	
PAF61	HRKKWFWAGPAHRKKWFWKDEL	22	2938.4	+5.2	10.6	−1.57	2	16		2	8	
PAF62	GHRKKWFWAGPAHRKKWFW	19	2509.9	+6.2	12.0	−1.46	2	16	8	2	4	
PAF63	SHRKKWFWAGPAHRKKWFW	19	2539.9	+6.2	12.0	−1.48	2	16		2	8	
PAF64	GHRKKWFWAGPAHRKKWFWKDEL	23	2995.4	+5.2	10.6	−1.52	2	32	8	2	8	
PAF65	SHRKKWFWAGPAHRKKWFWKDEL	23	3025.5	+5.2	10.6	−1.54	4	16	16	2	16	
PAF66	HRKKWFWHRKKWFW	14	2156.5	+6.2	12.0	−2.07						3
PAF67	HRKKWFWHRKKWFWKDEL	18	2642.1	+5.2	10.6	−2.01	4				16	
PAF68	GHRKKWFWHRKKWFW	15	2213.6	+6.2	12.0	−1.96	2		8		4	1
PAF69	SHRKKWFWHRKKWFW	15	2243.6	+6.2	12.0	−1.99	4				8	
PAF70	GHRKKWFWHRKKWFWKDEL	19	2699.1	+5.2	10.6	−1.92	2		8		16	2
PAF71	SHRKKWFWHRKKWFWKDEL	19	2729.1	+5.2	10.6	−1.94	2		8		16	1
PAF72	HRKKWFWAGPAHRKKWFWAGPAHRKKWFW	29	3818.5	+9.3	12.3	−1.39	1				4	
PAF73	HRKKWFWAGPAHRKKWFWAGPAHRKKWFWKDEL	33	4304.0	+8.3	11.2	−1.44	2	16		2	8	
PAF74	GHRKKWFWAGPAHRKKWFWAGPAHRKKWFW	30	3875.5	+9.3	12.3	−1.36	1	16	8		8	
PAF75	SHRKKWFWAGPAHRKKWFWAGPAHRKKWFW	30	3905.5	+9.3	12.3	−1.37	1				8	
PAF76	GHRKKWFWAGPAHRKKWFWAGPAHRKKWFW-KDEL	34	4361.1	+8.3	11.2	−1.41	1	16	4	2	4	
PAF77	SHRKKWFWAGPAHRKKWFWAGPAHRKKWFWKDEL	34	4391.1	+8.3	11.2	−1.42	1	16	4	2	4	1
PAF78	HRKKWFWHRKKWFWHRKKWFW	21	3225.8	+9.3	12.3	−2.07						3
PAF79	HRKKWFWHRKKWFWHRKKWFWKDEL	25	3711.3	+8.3	11.2	−2.02						3
PAF80	GHRKKWFWHRKKWFWHRKKWFW	22	3282.9	+9.3	12.3	−2.00	4				4	1
PAF81	SHRKKWFWHRKKWFWHRKKWFW	22	3312.9	+9.3	12.3	−2.01						3
PAF82	GHRKKWFWHRKKWFWHRKKWFWKDEL	26	3768.4	+8.3	11.2	−1.96	2				8	2
PAF83	SHRKKWFWHRKKWFWHRKKWFWKDEL	26	3798.4	+8.3	11.2	−1.98	2				4	2
PAF102	GHRKKWFWAGPARRKKWFWAGPAWRKKWFW	30	3943.6	+10.1	12.5	−1.32	1	16	8	2	8	

[a] The L-amino acid sequence is shown as single letter code. The six amino acid residues of the PAF26 sequence are underlined

[b] Molecular weight (MW), theoretical pI, and grand average of hydropathicity (GRAVY) index were estimated by the ProtParam tool (www.expasy.org)

[c] Net charge estimated at pH 7

[d] MIC value for each peptide and fungus combination (*Pdig*, *P. digitatum*; *Mory*, *M. oryzae*; *Foxy*, *F. oxysporum*; *Bcin*, *B. cinerea*). Peptide concentrations used with fungi were serial 2-fold dilutions from 32 μM. Blank cells denote peptide-microorganism combinations that were not tested

[e] MIC value for each peptide (peptide concentrations used with *E. coli* were serial 2-fold dilutions from 128 μM). Blank cells denote peptides not tested

[f] Solubility index (SI) recorded under the assay conditions (see main text for details). Blank cells indicate no turbidity in LB

Results

Concatemerization of antifungal PAF peptides results in increased antimicrobial activity

PAF54 (HRKKWFW) is a heptapeptide derived from PAF26 with an extension of one histidine residue at the N-terminus that gives optimal ratio of antimicrobial activity to nonspecific toxicity (Muñoz et al. 2007a, b). A total of 30 PAF peptides from 7 to 34 amino acid residues that include concatemers with tandem di- and tri-repeats of PAF54 were designed (Table 1), similarly to previous derivatives of the peptide BP100 (Badosa et al. 2013). The peptides were all possible combinations containing one, two, or three units of PAF54; interlinked or not with the AGPA hinge as a spacer and stabilization motif described previously (Badosa et al. 2013); with or without a KDEL fragment at the C-terminus as a signal for retention of peptides in the ER (Coca et al. 2006); and with either G or S residues at the N-terminus as an imprint of a specific protease processing site (Carrington and Dougherty 1988).

The peptides were tested for in vitro growth inhibition against the filamentous phytopathogenic fungi *P. digitatum*, *M. oryzae*, *F. oxysporum*, and *B. cinerea*, and a laboratory strain of *E. coli* (Fig. 1 and Table 1). These experiments demonstrated that double repeats of PAF (so called diPAFs) reduced the MIC value (i.e., increased the antimicrobial activity) 4 to 16-fold depending on the microorganism, while the addition of an additional PAF unit in a triPAF sequence only had at most a 2-fold increase of activity over the diPAFs. An exception was the activity toward *M. oryzae* because the increase of activity in any of the tandem sequences was not as high as with other microorganisms. In a previous study, this fungus also showed a qualitatively different sensitivity profile to different PAF heptapeptides (Muñoz et al. 2007b).

As expected, neutral additions of either G or S residues at the N-terminus did not affect the activity. The C-terminal addition of the KDEL sequence reduced 2-fold the activity in the monomeric peptides but had no significant effect in the di- or tri-PAF peptides. This result is likely due to the impact that the −1 net charge of KDEL (see Table 1), since cationic charge is critical for the initial attraction and binding of PAF peptides to the fungal surface (Muñoz et al. 2013b)

A positive effect was observed upon the addition of the AGPA hinge. DiPAFs and triPAFs without the AGPA tend to precipitate in some media such as the LB used in the antibacterial activity assays, as indicated by SI values above zero (Table 1), and in general do not dissolve as easily in aqueous buffers as the monomeric PAFs do. This effect was exemplified by PAF66 (Table 1); addition of G or S at the N-terminus (as in PAF68 and PAF69) or KDEL at the C-terminus (PAF67) increased solubility (i.e., reduced the SI). The effect of these additions was lost in the case of the triPAFs (compared with peptides PAF78 to PAF83). However, the insertion of the AGPA hinge between each PAF unit showed a very significant increase in solubility of both the diPAF and triPAF sequences.

Based on these observations, monoPAFs PAF54, PAF56, and PAF58; diPAFs PAF62 and PAF64; and triPAFs PAF74 and PAF76 were selected for further characterization as the most representative PAF concatemers described in the first part of the study.

Absence of hemolytic activity of PAF concatemers

An assay to determine the nonspecific toxicity of peptides to eukaryotic cells is the ability to lyse human red blood cells (erythrocytes). PAF26 is nonhemolytic to erythrocytes under conditions at which other cytolytic AMP such as melittin are (Muñoz et al. 2006). We determined the hemolytic activity of the selected PAF peptides at different concentrations, from to 2 up to 250 μM (i.e., approximately 100 times the completely inhibitory activity against *P. digitatum*) (Fig. 2). In these experiments, additional synthetic peptides were included as controls: the cytolytic peptide melittin from honeybee (Blondelle and Houghten 1991), the synthetic heptapeptide 77-3 that was identified by rational design (Gonzalez et al. 2002), and the P113 that is an active fragment of the antifungal histatin 5 and also a cell penetrating antifungal peptide (Jang et al. 2008).

As expected, the hemolytic peptide melittin caused more than 75 % hemolysis even at concentrations as low as 2 μM (Fig. 2). The peptide 77-3 showed an intermediate behavior, while the fragment P113 and the PAF peptides showed no hemolysis even at 250 μM, with values close to the control with no peptide added (<5 %). This result demonstrates that tandem repetition of PAF sequences does not have incidence on the very low hemolytic activity of the PAF peptides, confirming that these have very low nonspecific cell lytic activity and toxicity.

Concatemerization diminishes the fungicidal activity of PAF peptides against spores of *P. digitatum*

A distinctive property of PAF26 is its fungicidal activity against quiescent spores (Muñoz et al. 2007a). There are AMPs such as melittin that have fungistatic activity similar to PAF26 but that are not fungicidal against conidia of *P. digitatum*. Fungicidal activity of the selected PAF peptides was determined (Fig. 3). Interestingly, it was observed that fungicidal activity decreased with the increase of size and therefore goes in the opposite direction of the improvement of fungistatic activity observed with concatemerization. While monoPAFs are more than 90 % fungicidal at 16 μM, triPAF peptides are 60–70 % fungicidal at 64 μM. In these

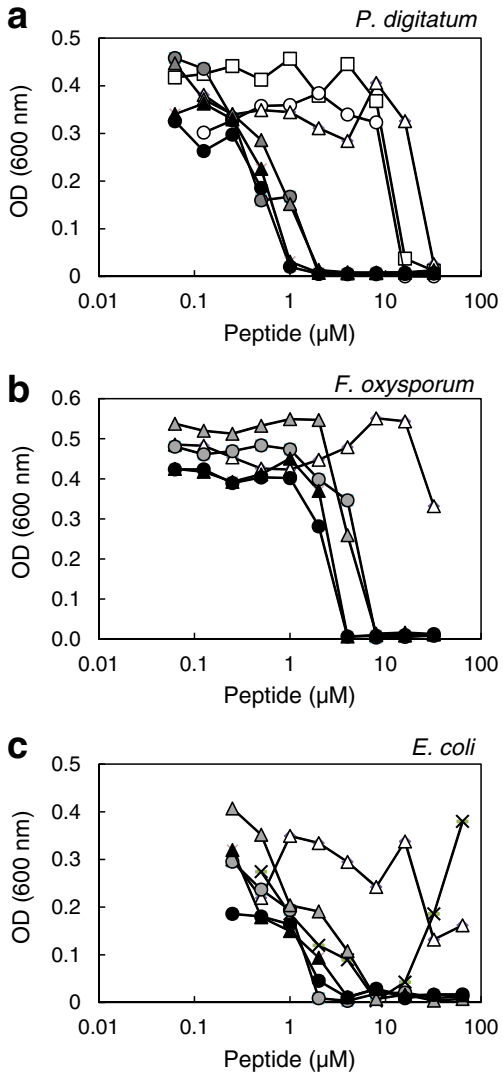

Fig. 1 Dose-response curves of in vitro growth inhibition of *P. digitatum* (**a**), *F. oxysporum* (**b**), and *E. coli* (**c**) by the synthetic peptides: PAF54 (*white squares*), PAF56 (*white circles*), PAF58 (*white triangles*), PAF62 (*gray circles*), PAF64 (*gray triangles*), PAF70 (*black crosses*), PAF74 (*black circles*), and PAF76 (*black triangles*). For clarity, note that not all the peptides are shown in each panel, that *triangles* indicate KDEL containing peptides, and that *colors* indicate monoPAFs (*white*), diPAFs (*gray*), or triPAFs (*black*). Dose-response curves show mean OD_{600} values of triplicate samples after 48 h of growth. The SD was less than 10 % of the mean in all the treatments. The peptide PAF70 (*black crosses*) is shown in **c** to illustrate the precipitation that occurred at high peptide concentration in some media such as the LB used in the antibacterial activity assays (see Table 1 and text for further details)

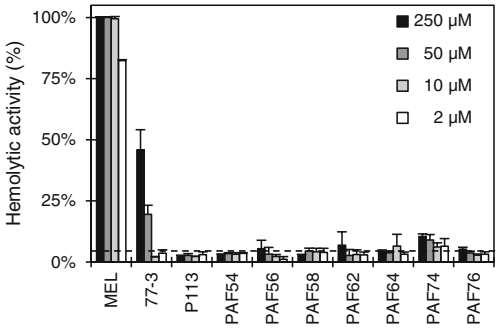

Fig. 2 Hemolytic activity of synthetic peptides. The peptides indicated were used at the concentrations indicated in the legend to assay their hemolytic activity. The hemolytic activity is given as the mean ± SD of the percentage of human erythrocyte hemolysis (three replicas), as compared with the positive control in the presence of the detergent Triton X-100 (100 % hemolysis). The *stripped line* marks the value of the background hemolysis in the negative control with no peptide added (value 4.8 %)

experiments, the triPAF peptide PAF102 (see below) was introduced and showed a behavior similar to PAF74 or PAF76.

Resistance of PAF peptides to proteolytic degradation

The in vitro stability of the peptides was determined by incubation with proteinase K at different times (Ferre et al. 2006) and RP-HPLC analysis of the resultant digests (Fig. 4). The monomeric peptide PAF56 was remarkably resistant to protease degradation since treatment with high doses of proteinase K (5 μg/mL) did not result in significant degradation after 120-min incubation. The monoPAF (PAF56/PAF58), diPAF (PAF62/64), and triPAF (PAF74/PAF76) couples of peptides differed only in the C-terminal addition of the KDEL sequence. All the peptides that have the KDEL were more susceptible to degradation than their counterparts of the same n-mer size (Fig. 4). RP-HPLC chromatograms demonstrated that the degradation of the KDEL-containing peptides did not result in the precise removal of this sequence, because none of the resultant fragments coeluted with the corresponding non-KDEL peptides (Supplementary Fig. S1). Interestingly, the size increase reduced the detrimental effect of the KDEL sequence on stability since the triPAF (PAF76) and diPAF (PAF64) were increasingly more resistant than PAF58 (Fig. 4).

PAF102 is internalized by fungal cells in an energy-dependent manner

Based on the previous data, we designed a new triPAF sequence (PAF102, Table 1). PAF102 is a two residue substitution of PAF74 in such a way that the second and third PAF units are modified in their first amino acid residue from PAF54 (HRKKWFW, the substituted residue is underlined) to the previously described heptapeptides PAF38 (RRKKWFW) (Muñoz et al. 2007a, b) and PAF42/PAF104 (WRKKWFW) (Muñoz et al. 2007b; Rebollar and López-García 2013). The rationale was to broaden and enhance the antifungal activity since PAF38 and PAF42/PAF104 have subtle differences in their activity profiles. However, the inhibitory and fungicidal activities of PAF74 and PAF102 did not differ in any of the microorganisms tested (Table 1, Fig. 3 and data not shown).

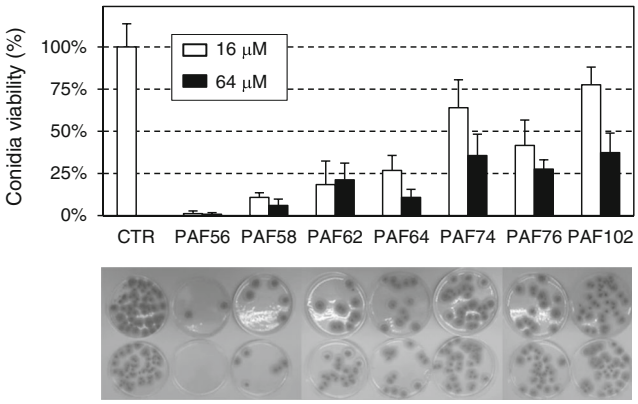

Fig. 3 Fungicidal activity of synthetic peptides. The graph at the top shows the viability of *P. digitatum* conidia after exposure to different peptides at the concentrations indicated in the legend. Data are the mean ± SD of the percentage of conidia viability after exposure to peptides (three replicas), as compared with the control (CTR) of no peptide added. The images at the bottom show representative plates of conidia viability exposed to the peptides at 16 μM

Experiments were designed to determine whether PAF102 showed cell penetration properties as PAF26. In addition, these experiments were conducted with an additional fungus (*F. proliferatum*) in order to broad the repertoire of fungi that have exhibited sensitivity to PAF peptides and in which cell penetration has been demonstrated. PAF102 inhibited the growth of *F. proliferatum* with a MIC value of 5 μM (Fig. 5). The MIC value of the fluorescent PAF102 labeled with rhodamine (TMR-PAF102) did not differ from unlabeled peptide (Fig. 5). A genetically modified strain of *F. proliferatum* that accumulates the fluorescent GFP protein at the cytosol was demonstrated to be as sensitive as the parental strain to TMR-PAF102 (Fig. 5) and PAF102 (data not shown).

The interaction of TMR-PAF102 with GFP-tagged *F. proliferatum* was followed by time-lapse live-cell imaging using confocal fluorescence microscopy (Fig. 6). Initially (up to 15 min), the red signal from the peptide located at the surface of the fungal cell (Fig. 6a, b), at the outermost layers of the CFW-stained fungal cell wall (Fig. 6f), similarly to results reported with PAF26 and *N. crassa* (Muñoz et al. 2012). The cell cytosol was filled with the green GFP signal and devoid of detectable red signal from the peptide. Interestingly, at early times, the peptide located first and in higher concentration at the envelope of the conidia (as seen in Fig. 6a, f) and not at the cell wall of the emerging germ tube. From 30 min, PAF102 started to accumulate in vacuoles within cells that did not present any sign of cell deterioration (Fig. 6c). At later stages, the peptide was transported out of the vacuoles and filled the cytosol (Fig. 6d), being distributed throughout the cell interior (Fig. 6e); at this phase, the cells presented high vacuolization and cytosolic granules indicative of cell deterioration and death. Some of these granules presented strong red labeling. These observations are fully consistent with previous data describing the interaction, internalization, and killing produced by PAF26 on *P. digitatum*, *N. crassa*, and *S. cerevisiae* (Harries et al. 2013; Muñoz et al. 2006, 2012, 2013b).

It was previously demonstrated that PAF26 internalization into *N. crassa* was energy-dependent (Muñoz et al. 2012). Sodium azide (NaN_3) treatment can be used to inhibit ATP production and thus energy-dependent processes. Pretreatment of *F. proliferatum* conidia with a sublethal concentration of NaN_3 abolished the internalization of PAF102 into *F. proliferatum* (Fig. 7). In the untreated control (Fig. 7a), the interaction and internalization of the labeled PAF102 was similar to the former experiments: the peptide interacted predominantly with the conidial wall and was then internalized to kill the germ tube cells, which showed granules of labeled material. Blockage of PAF102 internalization by NaN_3 treatment resulted in a homogeneous distribution of the peptide signal all along the cell wall of the germ tube, which stayed with no signs of cell killing or degradation even after long times of exposure (80 min) (Fig. 7b and data not shown).

Discussion

The peptide PAF26 is a model CP-AMP that has a dynamic antifungal mechanism of action involving at least three necessary but not sufficient sequential steps (Muñoz et al. 2013a, b): (i) peptide interaction with the fungal cell wall (Bou Zeidan

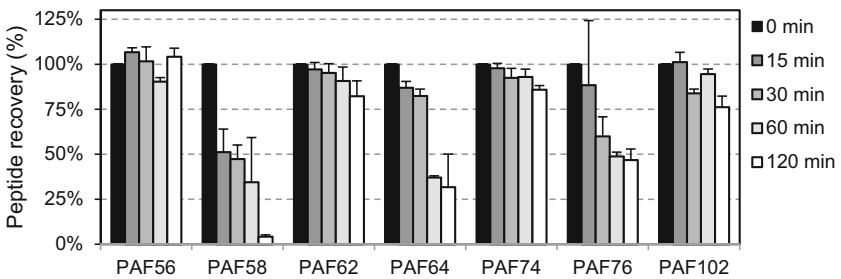

Fig. 4 Kinetics of peptide degradation in the presence of proteinase K. The graph shows the percentage recovery of the input peptides (5 μM) as mean ± SD of two replicates, determined by the resulting chromatographic peak area of the corresponding peptide after treatment with proteinase K (5 mg/mL) for different times (min) (see Supplementary Fig. S1 for representative RP-HPLC chromatograms)

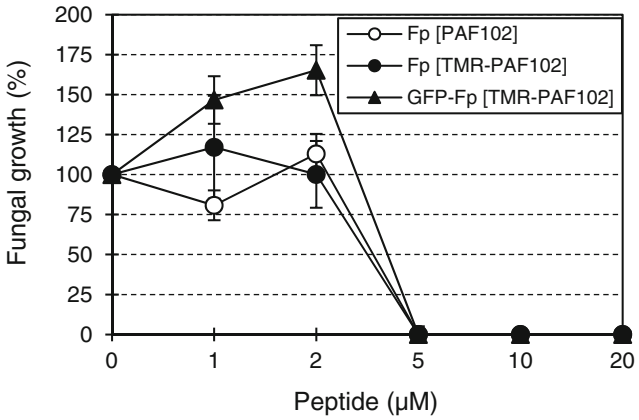

Fig. 5 In vitro growth inhibition of *F. proliferatum* by PAF102. The graph shows the percentage of fungal growth at different concentrations of peptides after 48-h incubation. The *white circles* represent the growth of *F. proliferatum* (Fp) after treatment with PAF102, the *black circles* after treatment with the labeled peptide TMR-PAF102, and the *black triangles* the effect of TMR-PAF102 on the growth of the GFP-tagged *F. proliferatum* (GFP-Fp). Data are mean ± SD of triplicate samples

et al. 2013; Harries et al. 2013), (ii) the subsequent endocytic-like internalization and accumulation in endosomes (Muñoz et al. 2012), and (iii) a series of complex and specific intracellular effects that include extrusion from endosomes and synthesis of reactive oxygen and nitric species (Carmona et al. 2012), and whose relationship with fungal death is still unclear. This study shows that concatemerization of the PAF26 sequence results in increased antifungal and antibacterial inhibitory activity of peptides, among which energy-dependent cell penetration into fungal cells is demonstrated in the example of PAF102. These observations are of high interest in the future development of PAF-based antimicrobial molecules.

MIC values of PAF concatemers against the filamentous fungi *P. digitatum* and *B. cinerea* were lowered to the range of 1-2 μM (Table 1 and Fig. 1). A significant reduction of the MIC value was also observed for *F. oxysporum* and *F. proliferatum*. Our study shows that the kinetics of the interaction and killing of *F. proliferatum* by PAF102 (Figs. 6 and 7) is markedly similar to that of *P. digitatum* or *N. crassa* by PAF26 (Muñoz et al. 2012, 2013b). Therefore, increase of activity is likely a consequence of the molar increase of physically linked AMP units per molecule of peptide, and not of any significant change in the mechanism of action. Increased antimicrobial activity was also associated with longer antifungal peptides in the case of the concatemer series of (RW) and (KW) dimeric peptides (Gopal et al. 2012) or of a tetramer branched derivative of B4010 (RGRKVVRR) (Lakshminarayanan et al. 2014), as well as in the antibacterial repeats of BP100 (Badosa et al. 2013), although no mechanistic data were reported in these studies.

A different result was found in the case of the rice blast fungus *M. oryzae*, since no significant improvement of activity of diPAFs or triPAFs was observed. For unknown reasons,

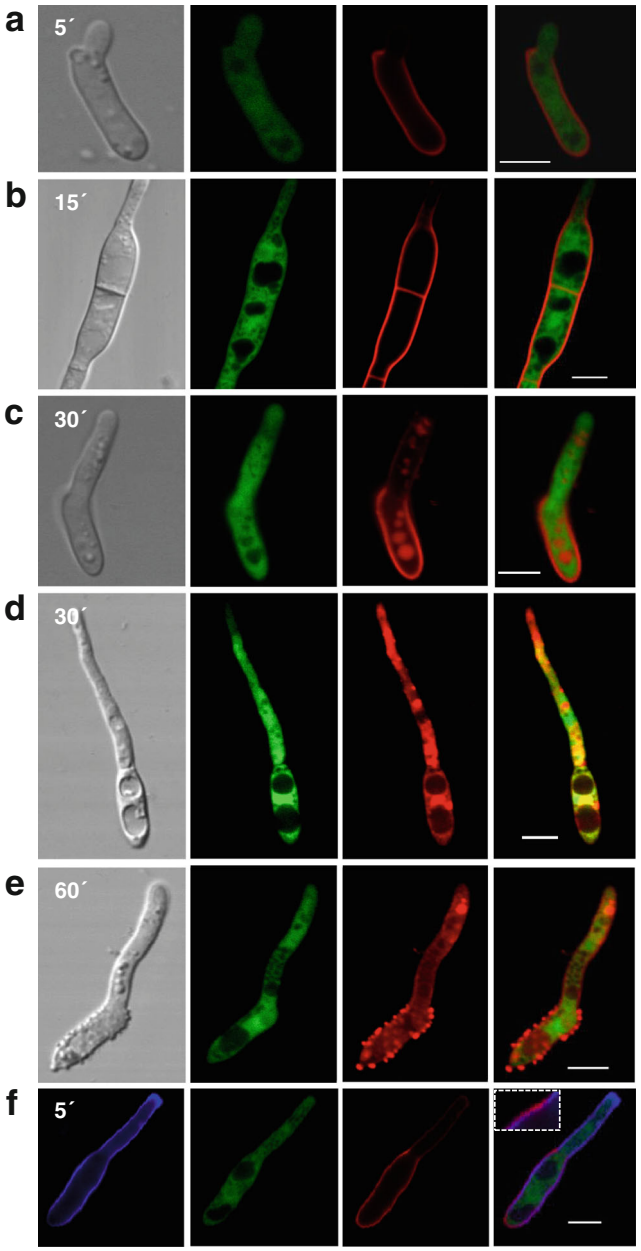

Fig. 6 Confocal fluorescence microscopy analyses of the interaction of TMR-PAF102 with GFP-tagged *F. proliferatum*. **a**–**e** Fungal germ tubes treated with 5 μM of TMR-PAF102 were visualized after the different times (min) of treatment shown in the *left column* images. *From left to right*, the images in columns show the bright field images, green GFP signal from GFP-Fp, red TMR signal from TMR-PAF102, and the colocalization of the latter two, from the same field. In **f**, an additional costaining with the cell wall selective dye CFW was conducted and the leftmost image shows the blue signal from CFW. The *rightmost image* shows the colocalization of the three signals, and the *inset* is an enlargement to illustrate the location of the peptide at the outer layer of the cell wall. *Bar*, 5 μm

M. oryzae is more tolerant than any other filamentous fungi tested to the growth inhibitory activity of peptides from the PAF series (Muñoz et al. 2007b). The lack of improvement with concatemerization reinforces the hypothesis that the

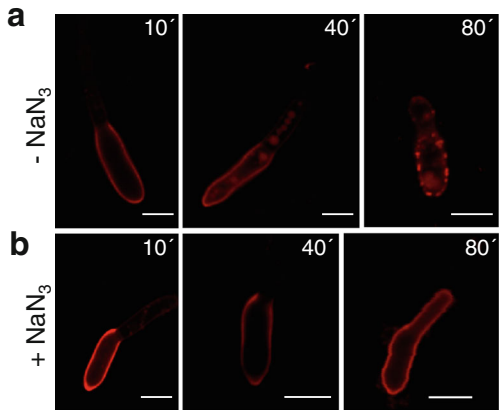

Fig. 7 PAF102 internalization into GFP-*F. proliferatum* is energy-dependent. Representative images of fungus not pretreated (**a**) or pretreated with NaN_3 for 15 min (**b**), at different times (min) after treatment with 5 μM TMR-PAF102. *Bar*, 5 μm

determinants of susceptibility to PAF peptides are different in this fungus. It was also demonstrated that the PAF104 (WRKKWFW) and other heptapeptides derived from PAF26 inhibited the *M. oryzae* appressorium formation rather than fungal growth (Rebollar and López-García 2013; Rebollar et al. 2014). Consistent with a lack of effect on *M. oryzae* growth, the inclusion of the PAF104 sequence as the third PAF unit in PAF102 did not enhance the inhibitory activity of triPAFs toward *M. oryzae*.

PAF26 and PAF26-derived monomeric peptides are selective against filamentous fungi, but also show reduced activity against bacteria and yeast (Muñoz et al. 2007b). Concatemerization brought the MIC value of the PAF peptides against the bacteria *E. coli* below 10 μM, while maintaining the low cell lytic activity (as assayed by hemolysis) of the monoPAFs, and therefore reveals the potential of PAF26-derived peptides also as antibacterial antibiotics in addition to their previously known antifungal activity. Nonlytic antibacterial mechanisms of action have been described for short AMPs (Marcos and Gandía 2009; Scocchi et al. 2011; Wilmes et al. 2011). Although the precise antibacterial mechanism of concatemeric PAFs needs to be studied in detail, their lack of hemolytic activity indicates that they do not act simply by membrane permeabilization. In the case of filamentous fungi and yeast, the activity of PAF26 is mediated by the initial interaction with the fungal cell wall and cell wall glycoproteins (Bou Zeidan et al. 2013; Harries et al. 2013). Therefore, the role of the bacterial cell wall in the activity of PAF concatemers should be examined in the future for the characterization of the antibacterial activity.

The partial loss of fungicidal activity against conidia of the concatemers (Fig. 3) indicates that the peptide interaction is different in conidia and mycelium. This might reflect the importance of the initial interaction of peptides with the cell wall. The cell wall of conidia and hyphal cells presents differences in structure and composition, exemplified in the repertoire of hydrophobins that confer specific properties to conidia (Bayry et al. 2012; Latgé 2007). Our microscopy data shows that PAF102 interacts better with the conidial surface than with the emerging germ tube (Figs. 6 and 7). Similar results were observed in the case the fluorescently labelled PAF62 or PAF64 (data not shown). A high affinity interaction could result in the sequestration of the peptide at the cell surface that could limit the internalization and hence the cell killing, similarly to the inactive PAF96 derivative (RKKAAA) that strongly interacts with the cell wall, but does not progress into the cell and therefore does not kill the fungal cell (Muñoz et al. 2013b). Nevertheless, the reduced fungicidal activity would be counterbalanced by the increased growth inhibition of the concatemers (fungistatic activity) once the fungal spores germinate.

We have demonstrated that the monomeric PAF54 is markedly resistant to protease degradation in vitro. Proteinase K is commonly used in in vitro protein stability assays for its broad specificity. The predominant site of cleavage is the peptide bond adjacent to the carboxyl group of aliphatic or aromatic amino acids, and therefore, the PAF primary structure should be susceptible to proteinase K degradation. Our findings indicate that higher order structures make PAF peptides resistant to degradation. Size increase of PAF-derived peptides should further enhance their stability when they are produced through biotechnology in living cell factories, as proposed for other AMPs (Badosa et al. 2013; Ingham and Moore 2007; Nadal et al. 2012). However, peptide designs might have important effects on peptide stability (Fig. 4). This is highlighted with the inclusion of the KDEL ER retention signal used for in planta expression (Coca et al. 2006), which unexpectedly targeted the PAF peptides for degradation. This effect might be specific of PAF sequences since it has not been reported yet for other peptides. It remains to be determined to which extent the properties of the PAF concatemers described in this study are also observed in the case of peptides produced in cell biofactories.

Acknowledgments This work was funded by grants EUI2008-03619 and EUI2008-03769 from "Ministerio de Ciencia e Innovación" (MICINN, Spain). EH was a recipient of a scholarship within the JAE PRE-DOC program (CSIC, EU FEDER funds). We acknowledge the technical assistance of M. José Pascual and Montse Amenós with confocal microscopy.

References

Badosa E, Moiset G, Montesinos L, Talleda M, Bardaji E, Feliu L, Planas M, Montesinos E (2013) Derivatives of the antimicrobial peptide BP100 for expression in plant systems. PLoS ONE 8:e85515

Bayry J, Aimanianda V, Guijarro JI, Sunde M, Latgé JP (2012) Hydrophobins-unique fungal proteins. PLoS Pathog 8:e1002700

Blondelle SE, Houghten RA (1991) Hemolytic and antimicrobial activities of the 24 individual omission analogs of melittin. Biochemistry 30:4671–4678

Bou Zeidan M, Carmona L, Zara S, Marcos JF (2013) *FLO11* gene is involved in the interaction of flor strains of *Saccharomyces cerevisiae* with a biofilm-promoting synthetic hexapeptide. Appl Environ Microbiol 79:2023–2032

Bundó M, Montesinos L, Izquierdo E, Campo S, Mieulet D, Guiderdoni E, Rossignol M, Badosa E, Montesinos E, San Segundo B, Coca M (2014) Production of cecropin A antimicrobial peptide in rice seed endosperm. BMC Plant Biol 14:102

Campos-Soriano L, San Segundo B (2009) Assessment of blast disease resistance in transgenic *PRms* rice using a *gfp*-expressing *Magnaporthe oryzae* strain. Plant Pathol 58:677–689

Carmona L, Gandía M, López-García B, Marcos JF (2012) Sensitivity of *Saccharomyces cerevisiae* to the cell-penetrating antifungal peptide PAF26 correlates with endogenous nitric oxide (NO) production. Biochem Biophys Res Commun 417:56–61

Carrington JC, Dougherty WG (1988) A viral cleavage site cassette: Identification of amino acid sequences required for tobacco etch virus polyprotein processing. Proc Natl Acad Sci U S A 85:3391–3395

Coca M, Bortolotti C, Rufat M, Peñas G, Eritja R, Tharreau D, Martínez del Pozo A, Messeguer J, San Segundo B (2004) Transgenic rice plants expressing the antifungal AFP protein from *Aspergillus giganteus* show enhanced resistance to the rice blast fungus *Magnaporthe grisea*. Plant Mol Biol 54:245–259

Coca M, Peñas G, Gómez J, Campo S, Bortolotti C, Messeguer J, San Segundo B (2006) Enhanced resistance to the rice blast fungus *Magnaporthe grisea* conferred by expression of a cecropin A gene in transgenic rice. Planta 223:392–406

Company N, Nadal A, La Paz JL, Martínez S, Rasche S, Schillberg S, Montesinos E, Pla M (2014) The production of recombinant cationic α-helical antimicrobial peptides in plant cells induces the formation of protein bodies derived from the endoplasmic reticulum. Plant Biotechnol J 12:81–92

Cotter PD, Hill C, Ross RP (2005) Bacteriocins: developing innate immunity for food. Nat Rev Microbiol 3:777–788

Chen X, Stone M, Schlagnhaufer C, Romaine CP (2000) A fruiting body tissue method for efficient *Agrobacterium*-mediated transformation of *Agaricus bisporus*. Appl Environ Microbiol 66:4510–4513

De Lucca AJ, Walsh TJ (1999) Antifungal peptides: novel therapeutic compounds against emerging pathogens. Antimicrob Agents Chemother 43:1–11

De Souza Cândido E, e Silva Cardoso MH, Sousa DA, Viana JC, De Oliveira-Júnior NG, Miranda V, Franco OL (2014) The use of versatile plant antimicrobial peptides in agribusiness and human health. Peptides 55:65–78

Dempsey CE (1990) The actions of melittin on membranes. Biochim Biophys Acta 1031:143–161

Di Pietro A, Roncero MIG (1996) Endopolygalacturonase from *Fusarium oxysporum* f sp *lycopersici*: Purification, characterization, and production during infection of tomato plants. Phytopathology 86:1324–1330

Duncan VMS, O'Neil DA (2013) Commercialization of antifungal peptides. Fungal Biol Rev 26:156–165

Ferre R, Badosa E, Feliu L, Planas M, Montesinos E, Bardají E (2006) Inhibition of plant-pathogenic bacteria by short synthetic cecropin A-melittin hybrid peptides. Appl Environ Microbiol 72:3302–3308

Gonzalez CF, Provin EM, Zhu L, Ebbole DJ (2002) Independent and synergistic activity of synthetic peptides against thiabendazole-resistant *Fusarium sambucinum*. Phytopathology 92:917–924

Gopal R, Na H, Seo CH, Park Y (2012) Antifungal activity of (KW)n or (RW)n peptide against *Fusarium solani* and *Fusarium oxysporum*. Int J Mol Sci 13:15042–15053

Hancock REW, Sahl HG (2006) Antimicrobial and host-defense peptides as new anti-infective therapeutic strategies. Nat Biotechnol 24:1551–1557

Harries E, Carmona L, Muñoz A, Ibeas JI, Read ND, Gandía M, Marcos JF (2013) Genes involved in protein glycosylation determine the activity and cell internalization of the antifungal peptide PAF26 in *Saccharomyces cerevisiae*. Fungal Genet Biol 58–59:105–115

Ingham AB, Moore RJ (2007) Recombinant production of antimicrobial peptides in heterologous microbial systems. Biotechnol Appl Biochem 47:1–9

Jang WS, Li XWS, Sun JNN, Edgerton M (2008) The P-113 fragment of histatin 5 requires a specific peptide sequence for intracellular translocation in *Candida albicans*, which is independent of cell wall binding. Antimicrob Agents Chemother 52:497–504

Jenssen H, Hamill P, Hancock REW (2006) Peptide antimicrobial agents. Clin Microbiol Rev 19:491–511

Lakshminarayanan R, Liu S, Li J, Nandhakumar M, Aung TT, Goh E, Chang JYT, Saraswathi P, Tang C, Safie SRB, Lin LY, Riezman H, Lei Z, Verma CS, Beuerman RW (2014) Synthetic multivalent antifungal peptides effective against fungi. PLoS ONE 9:e87730

Latgé JP (2007) The cell wall: A carbohydrate armour for the fungal cell. Mol Microbiol 66:279–290

López-García B, Pérez-Payá E, Marcos JF (2002) Identification of novel hexapeptides bioactive against phytopathogenic fungi through screening of a synthetic peptide combinatorial library. Appl Environ Microbiol 68:2453–2460

López-García B, Veyrat A, Pérez-Payá E, González-Candelas L, Marcos JF (2003) Comparison of the activity of antifungal hexapeptides and the fungicides thiabendazole and imazalil against postharvest fungal pathogens. Int J Food Microbiol 89:163–170

López-García B, Ubhayasekera W, Gallo RL, Marcos JF (2007) Parallel evaluation of antimicrobial peptides derived from the synthetic PAF26 and the human LL37. Biochem Biophys Res Commun 356:107–113

López-García B, San Segundo B, Coca M (2012) Antimicrobial peptides as a promising alternative for plant disease protection. In: Rajasekaran K, Cary JW, Jaynes J, Montesinos E (eds) Small wonders: Peptides for disease control. American Chemical Society, Washington, DC, pp 263–294

Marcos JF, Gandía M (2009) Antimicrobial peptides: to membranes and beyond. Expert Opin Drug Discov 4:659–671

Marcos JF, Muñoz A, Pérez-Payá E, Misra S, López-García B (2008) Identification and rational design of novel antimicrobial peptides for plant protection. Annu Rev Phytopathol 46:273–301

Montesinos E, Bardaji E (2008) Synthetic antimicrobial peptides as agricultural pesticides for plant-disease control. Chem Biodivers 5:1225–1237

Muñoz A, López-García B, Marcos JF (2006) Studies on the mode of action of the antifungal hexapeptide PAF26. Antimicrob Agents Chemother 50:3847–3855

Muñoz A, López-García B, Marcos JF (2007a) Comparative study of antimicrobial peptides to control citrus postharvest decay caused by *Penicillium digitatum*. J Agric Food Chem 55:8170–8176

Muñoz A, López-García B, Pérez-Payá E, Marcos JF (2007b) Antimicrobial properties of derivatives of the cationic tryptophan-rich hexapeptide PAF26. Biochem Biophys Res Commun 354:172–177

Muñoz A, Marcos JF, Read ND (2012) Concentration-dependent mechanisms of cell penetration and killing by the *de novo* designed antifungal hexapeptide PAF26. Mol Microbiol 85:89–106

Muñoz A, Gandía M, Harries E, Carmona L, Read ND, Marcos JF (2013a) Understanding the mechanism of action of cell-penetrating antifungal peptides using the rationally designed hexapeptide PAF26 as a model. Fungal Biol Rev 26:146–155

Muñoz A, Harries E, Contreras-Valenzuela A, Carmona L, Read ND, Marcos JF (2013b) Two functional motifs define the interaction,

internalization and toxicity of the cell-penetrating antifungal peptide PAF26 on fungal cells. PLoS ONE 8:e54813

Nadal A, Montero M, Company N, Badosa E, Messeguer J, Montesinos L, Montesinos E, Pla M (2012) Constitutive expression of transgenes encoding derivatives of the synthetic antimicrobial peptide BP100: impact on rice host plant fitness. BMC Plant Biol 12: 159

Parachin NS, Mulder KC, Viana AAB, Dias SC, Franco OL (2012) Expression systems for heterologous production of antimicrobial peptides. Peptides 38:446–456

Piers KL, Brown MH, Hancock REW (1994) Improvement of outer membrane-permeabilizing and lipopolysaccharide-binding activities of an antimicrobial cationic peptide by C-terminal modification. Antimicrob Agents Chemother 38:2311–2316

Rebollar A, López-García B (2013) PAF104, a synthetic peptide to control rice blast disease by blocking appressorium formation in *Magnaporthe oryzae*. Mol Plant-Microbe Interact 26:1407–1416

Rebollar A, Marcos JF, López-García B (2014) Screening of a synthetic peptide combinatorial library to identify inhibitors of the appressorium formation in *Magnaporthe oryzae*. Biochem Biophys Res Commun 454:1–6

Scocchi M, Tossi A, Gennaro R (2011) Proline-rich antimicrobial peptides: converging to a non-lytic mechanism of action. Cell Mol Life Sci 68:2317–2330

Viana JFC, Dias SC, Franco OL, Lacorte C (2013) Heterologous production of peptides in plants: Fusion proteins and beyond. Curr Protein Pept Sci 14:568–579

Wang XJ, Wang XM, Teng D, Zhang Y, Mao RY, Wang JH (2014) Recombinant production of the antimicrobial peptide NZ17074 in *Pichia pastoris* using SUMO3 as a fusion partner. Lett Appl Microbiol 59:71–78

Wilmes M, Cammue BPA, Sahl HG, Thevissen K (2011) Antibiotic activities of host defense peptides: More to it than lipid bilayer perturbation. Nat Prod Rep 28:1350–1358

Zasloff M (2002) Antimicrobial peptides of multicellular organisms. Nature 415:389–395